Journal of Biomechanics 48 (2015) 644–650

Contents lists available at ScienceDirect

Journal of Biomechanics

journal homepage: www.elsevier.com/locate/jbiomech
www.JBiomech.com

How tibiofemoral alignment and contact locations affect predictions of medial and lateral tibiofemoral contact forces

Zachary F. Lerner [a,*], Matthew S. DeMers [b], Scott L. Delp [b], Raymond C. Browning [a,c]

[a] School of Biomedical Engineering, Colorado State University, Fort Collins, CO, USA
[b] Departments of Bioengineering and Mechanical Engineering, Stanford University, Stanford, CA, USA
[c] Department of Health and Exercise Science, Colorado State University, Fort Collins, CO, USA

ARTICLE INFO

Article history:
Accepted 26 December 2014

Keywords:
Tibiofemoral contact force
Walking
Musculoskeletal modeling
Joint loading
Osteoarthritis

ABSTRACT

Understanding degeneration of biological and prosthetic knee joints requires knowledge of the *in-vivo* loading environment during activities of daily living. Musculoskeletal models can estimate medial/lateral tibiofemoral compartment contact forces, yet anthropometric differences between individuals make accurate predictions challenging. We developed a full-body OpenSim musculoskeletal model with a knee joint that incorporates subject-specific tibiofemoral alignment (*i.e.* knee varus-valgus) and geometry (*i.e.* contact locations). We tested the accuracy of our model and determined the importance of these subject-specific parameters by comparing estimated to measured medial and lateral contact forces during walking in an individual with an instrumented knee replacement and post-operative genu valgum (6°). The errors in the predictions of the first peak medial and lateral contact force were 12.4% and 11.9%, respectively, for a model with subject-specific tibiofemoral alignment and contact locations determined through radiographic analysis, *vs.* 63.1% and 42.0%, respectively, for a model with generic parameters. We found that each degree of tibiofemoral alignment deviation altered the first peak medial compartment contact force by 51N (r^2=0.99), while each millimeter of medial-lateral translation of the compartment contact point locations altered the first peak medial compartment contact force by 41N (r^2=0.99). The model, available at www.simtk.org/home/med-lat-knee/, enables the specification of subject-specific joint alignment and compartment contact locations to more accurately estimate medial and lateral tibiofemoral contact forces in individuals with non-neutral alignment.

1. Introduction

Abnormal knee loads are implicated in tibiofemoral osteoarthritis (Sharma et al., 1998), which affects more than 12% of US adults (Dillon et al., 2006). The distribution of tibiofemoral contact forces between the medial and lateral compartments can be influenced by frontal-plane tibiofemoral alignment and affect degeneration of biological (Sharma et al., 2001) and prosthetic (Ritter et al., 1994) knees. The treatment of orthopedic disorders of the knee is likely to benefit from an improved understanding of the *in-vivo* knee loading environment during activities of daily living.

Musculoskeletal models allow researchers to investigate medial/lateral tibiofemoral contact forces during activities such as walking (Fregly et al., 2012; Morrison, 1970). Some modeling approaches require complex, multi-step analyses, or the use of both full-body gait models and finite element or contact models (Bei and Fregly, 2004; Hast and Piazza, 2013; Lin et al., 2010; Thelen et al., 2014; Yang et al., 2010). Finite element and contact models rely on an accurate representation of the articulating joint surfaces and require imaging techniques that may be unavailable or prohibitively expensive. Resolving the magnitudes of medial/lateral forces by approximating medial/lateral compartment points of contact is a promising approach for estimating contact forces (Gerus et al., 2013; Kumar et al., 2012; Winby et al., 2009); however, no open-source, full-body gait model contains knee joint definitions that allow direct computation of medial/lateral contact forces.

Predictions of medial/lateral tibiofemoral contact forces in an individual using a musculoskeletal model with generic geometry may be inaccurate when the model does not accurately represent the individual. The specification of certain subject-specific model parameters may improve accuracy (Gerus et al., 2013). Two parameters, frontal-plane tibiofemoral alignment and medial/lateral compartment contact locations, are likely to influence model-predicted medial/lateral compartment contact forces by altering how muscle forces and external loads pass relative to each compartment. Frontal-plane tibiofemoral alignment affects loading of the knee (Halder et al., 2012; Hsu et al., 1990; Hurwitz et al., 2002; Yang et al., 2010), and can vary

* Correspondence to: 220 Moby B Complex Colorado State University Fort Collins, CO 80523-1582. Tel.: +814 571 4616; fax: +970 491 0445.
E-mail address: Zach.Lerner@ColoState.edu (Z.F. Lerner).

http://dx.doi.org/10.1016/j.jbiomech.2014.12.049
0021-9290/

up to $\pm 3.75^{\circ}$ in individuals without obvious genu valgum-varum (Moreland et al., 1987). Existing modeling approaches have limitations that hinder the accurate representation of a subject's frontal-plane alignment; for example, generic models typically lack or constrain the frontal-plane motion of the knee (Gerus et al., 2013; Hast and Piazza, 2013; Kumar et al., 2012; Winby et al., 2009) and subject-specific models based on geometry determined from MRI or CT images are of non-weight-bearing limbs (Bei and Fregly, 2004; Gerus et al., 2013). In addition, when medial/lateral compartment contact is approximated through single points, the locations of these points influence how the tibiofemoral loads are distributed. It has been assumed that the medial/lateral compartment contact locations are centered at the midline of the femoral condyles (Winby et al., 2009) in biological knees or located at set distances from the joint center in prosthetic knees (Gerus et al., 2013), but variability in alignment and joint degeneration may alter these locations.

To address the need to calculate tibiofemoral loads accurately this study had three goals. The first was to develop a musculoskeletal model that accounts for differences in tibiofemoral alignment and contact locations and computes medial/lateral contact forces during walking. The second goal was to quantify the accuracy of knee contact force estimates made using generic geometry and subject-specific geometry by comparing these estimates to *in-vivo* measurements from an individual with an instrumented knee replacement and genu valgum. The third goal was to evaluate the effects of model-specified frontal-plane knee alignment and contact point locations on medial/lateral contact force predictions. The model, experimental data, and contact force predictions are freely available at www.simtk.org.

2. Methods

2.1. Model development

To compute medial and lateral tibiofemoral contact forces during walking we developed a model of the tibiofemoral joint in OpenSim (Delp et al., 2007) and incorporated it within a published full body musculoskeletal model (DeMers et al., 2014). The published model, designed for studying gait, was comprised of 18 body segments and 92 muscle-tendon actuators. Model degrees of freedom (DOF) included a ball-and-socket joint between the third and fourth lumbar vertebra, three translations and three rotations of the pelvis, a ball-and-socket joint at each hip, and revolute ankle and subtalar joints. In our model, the sagittal plane rotation and translations of the tibia and patella relative to the femur were identical to those specified by (Delp et al., 1990); however, we augmented the mechanism defining the tibiofemoral kinematics.

The tibiofemoral model introduced components for configuring frontal-plane alignment of the knee and for resolving distinct medial and lateral tibiofemoral forces. We introduced a distal femoral component body and a tibial plateau body (represented by CAD geometry of the instrumented implant, Fig. 1, pink) with orientation parameters for configuring frontal-plane alignment in the femur (θ_1) and tibia (θ_2). Between the femoral component and the tibial plateau, we defined a series of joints to characterize the tibiofemoral kinematics and medial/lateral load distribution. Firstly, the knee joint from Delp et al. (1990) defined the sagittal-plane rotations and translations of the knee between the femoral component and the sagittal articulation frame of reference (Fig. 1A, hidden, Fig. 1B, translucent). Secondly, two revolute joints connected the sagittal articulation frame to medial and lateral tibiofemoral compartments (Fig. 1, purple). The axes for these two revolute joints were perpendicular to the frontal-plane. Lastly, the medial and lateral compartments were welded at the anterioposterior mid-point of the tibial plateaus such that they remained fixed to the tibia while articulating with the surface of the femoral component during flexion-extension. The patella segment articulated with the femoral-condyle segment according to (DeMers et al., 2014). The quadriceps muscles wrapped around the patella before attaching to the tibial tuberosity to redirect the quadriceps forces along the line of action of the patellar ligament and allow the resultant tibiofemoral contact forces to be computed (DeMers et al., 2014).

In this knee mechanism, the medial and lateral revolute joints cannot resist frontal-plane moments individually. However, by acting in parallel, the two joints share all loads transmitted between the femur and tibia and resolve them as the medial and lateral contact forces required to balance the net reaction forces and frontal-plane moments across the tibiofemoral joint. Correspondingly, the knee remained a single DOF joint with motion only in the sagittal plane. The medial and lateral contact forces were computed and reported using the Joint Reaction Analysis in OpenSim (Steele et al., 2012).

2.2. Experimental data

We used experimental data from a subject with an instrumented knee replacement (right knee, male, age 83, mass 67 kg, height 1.72 m) to generate dynamic simulations of walking. These data have been made available by the Knee Load Grand Challenge (Fregly et al., 2012). Researchers collected kinematic, kinetic, and instrumented implant data simultaneously during over-ground walking. Validated regression equations were used to calculate separate medial and lateral tibiofemoral compartment contact forces from the instrumented knee joint (Meyer et al., 2001).

Established methods (Moreland et al., 1987) were used to quantify the frontal-plane alignment of the subject's right lower-extremity from a standing anterioposterior radiograph (Fig. 2). The angle formed between the intersection of the mechanical axes of the femur and tibia was used to specify subject-specific model alignment. To model lower-extremity alignment, θ_1 and θ_2 from Fig. 1 are each specified as one half of the varus-valgus alignment angle (180°–θ from Fig. 2). To estimate subject-specific medial/lateral compartment contact locations, we measured the distance between the centerline of the femoral implant component and the centerline of the tibial implant component using a higher resolution anterioposterior radiograph of the knee (Fig. 3). A measurement scale was established from the known width of the implant. Contact model predictions using *in-vivo* measurements of a similar implant have indicated an intercondylar distance of 40 mm (Zhao et al., 2007), and this distance has been used previously to inform model contact points (Gerus et al., 2013). Therefore, we maintained this intercondylar distance while shifting the medial/lateral contact locations medially by the distance (d) measured from the radiograph.

2.3. Varying tibiofemoral specificity in the musculoskeletal model

To isolate the effects of specifying each subject-specific parameter we conducted simulations with the following four conditions of our musculoskeletal model.

2.3.1. Fully-informed model

This model had subject-specific tibiofemoral alignment ($\theta = 174^{\circ}$) and contact locations informed through radiographic analysis. Medial compartment contact was located 23 mm medial of the knee joint center and lateral compartment contact was located 17 mm lateral of the knee joint center.

2.3.2. Uninformed model

Based on data from an instrumented implant contact model for a neutrally aligned lower-extremity (Zhao et al., 2007), and matching assumptions for an artificial knee implant made previously (Gerus et al., 2013), we specified the generic frontal-plane locations of the medial/lateral compartment structures 20 mm medial and lateral of the knee joint center. The tibiofemoral alignment for this model ($\theta = 180^{\circ}$) was maintained from skeletal geometry originally defined by (Delp et al., 1990).

2.3.3. Alignment-informed model

This model had subject-specific alignment ($\theta = 174^{\circ}$) but uninformed contact locations (20 mm medial and lateral of the joint center).

2.3.4. Contact-point-informed model

This model had subject-specific contact locations (medial compartment: 23 mm medial of the joint center, lateral compartment: 17 mm lateral of the joint center) but uninformed alignment ($\theta = 180^{\circ}$).

To investigate the effects of model-specified tibiofemoral alignment on model-predictions, we created contact-point-informed models with variable tibiofemoral alignment ranging from 0°–8° valgus, at 2° increments. To investigate the effects of model-specified medial/lateral compartment contact locations on model-predictions, we created alignment-informed models with variable medial/lateral contact point locations spanning reported translations (± 4 mm) at 2 mm increments with 40 mm inter-condylar distances.

2.4. Musculoskeletal simulation of walking

We used marker location data from anatomical landmarks collected during a standing calibration trial to scale our models in OpenSim. For each scaled model, we used OpenSim's inverse kinematics analysis, which minimized the errors between markers fixed to the model and experimentally measured marker trajectories (Delp et al., 2007), to determine the joint angles during four over-ground walking trials. Model kinematics were recalculated for every model condition while the ground reaction forces remained the same. Because muscle forces are the main determinant of compressive tibiofemoral contact forces (Herzog et al., 2003), variations in muscle activity greatly influence the magnitude and accuracy of knee joint contact force predictions (DeMers et al., 2014). We resolved individual muscle forces using a weighted static optimization approach that was calibrated to the

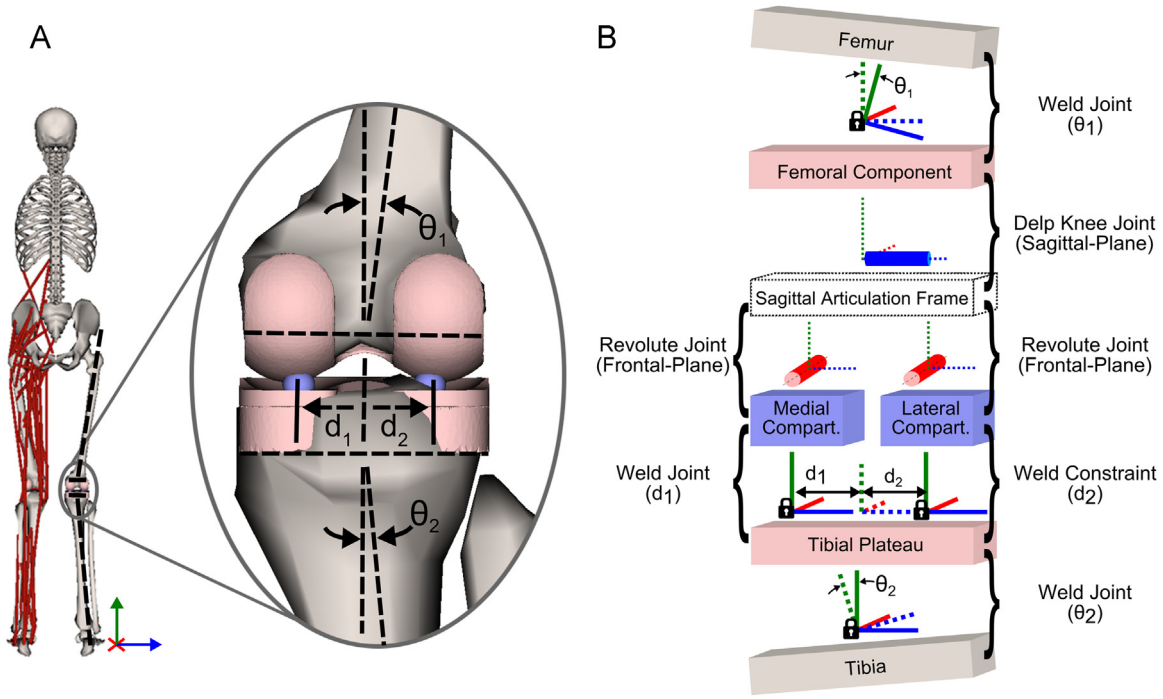

Fig. 1. Graphical (A) and schematic (B) depictions of the medial/lateral compartment joint structures in our musculoskeletal model. In both the graphic and schematic, the red axis is perpendicular to the frontal-plane, the green axis is perpendicular to the transverse-plane, and the blue axis is perpendicular to the sagittal-plane. The "Delp Knee Joint" defines the sagittal-plane tibiofemoral translations and rotations specified by (Delp et al., 1990) (blue cylinder in B). Two revolute joints (red cylinders), acting in the frontal-plane, connect the sagittal articulation frame (translucent) to both the medial and lateral compartments (purple). By acting in parallel, these two revolute joints share all loads transmitted between the femur and tibia and resolve the medial and lateral contact forces required to balance the net reaction forces and frontal-plane moments across the tibiofemoral joint. The medial compartment is fixed to the tibial plateau with a weld joint, and the lateral compartment is fixed to the tibial plateau with a weld constraint (black locks). Correspondingly, the knee remained a single DOF joint with articulation only in the sagittal plane. The locations of the medial and lateral compartments can be specified on a subject-specific basis (d_1 and d_2 in the inset graphic and schematic). Similarly, the model's tibiofemoral alignment can be specified (θ_1 and θ_2 in the inset graphic and schematic) by modifying the weld joint between the femur and femoral component and the weld joint between the tibial plateau and tibia.

subject (Lerner et al., 2013; Steele et al., 2012). The objective function minimized the sum of squared muscle activations while incorporating individual muscle weighting values using the method described by (Steele et al., 2012). We manually adjusted the weighting values by half-integers until the combined first and second peak error between the measured and predicted medial/lateral tibiofemoral contact force was minimized for this subject. Muscle weighting factors of 1.5 for the gastrocnemius, 2 for the hamstrings, and 1 for all other muscles in the model, resulted in the lowest combined medial/lateral first and second peak prediction errors for each of the model conditions. The same weighting factors were used across all model conditions.

We computed the forces in the medial/lateral compartment joint structures using OpenSim's JointReaction analyses (Steele et al., 2012), which determines the resultant forces and moments acting on each articulating joint structure from all muscle forces and external and internal loads applied to the model. Medial/lateral tibiofemoral contact forces were computed as the component of each resultant force acting normal to the tibial plateau.

We used the fully-informed model to verify the contact forces predicted by the medial/lateral joint structures by comparing the outputs from the JointReaction analysis to the medial/lateral contact forces determined from the well-established point-contact method (Winby et al., 2009). This method balances the forces and moments acting at the knee joint about medial/lateral tibiofemoral contact points based on the principle of static equilibrium. OpenSim's inverse dynamics tool was used to determine the external abduction-adduction moment, while the muscle analysis tool was used to determine individual muscle moment arms about the medial and lateral compartment joint structures. The contact forces acting on the medial/lateral joint structures of our OpenSim model, as reported from the JointReaction analysis, were identical to the medial/lateral tibiofemoral contact forces quantified using the point-contact method.

2.5. Statistical analysis

For each model condition, the contact force predictions for each walking trial were normalized to percent stance phase and averaged across stance phases to determine the mean and standard deviation. We calculated 95% confidence intervals to determine if statistically significant differences existed for first and second peak contact forces between model predictions and the *in-vivo* measurements, and to determine if significant differences existed between peak muscle forces. Regression analysis was used to determine the relationship between model-specified tibiofemoral alignment and contact point locations and first peak medial compartment forces. We also calculated the total (medial+lateral) root-mean-square errors (RMSE) between the predicted and measured contact forces. SigmaPlot, version 11.0 (Systat Software, Inc., San Jose, *CA*) was used to perform the statistical analyses.

3. Results

The fully-informed model had the best prediction accuracy. The alignment-informed model resulted in more accurate predictions than the contact-point-informed model; the least accurate was the uniformed model (Figs. 4 and 5). Specifying subject-specific alignment and contact locations improved prediction accuracy by decreasing the contact force in the medial compartment and increasing the contact force in the lateral compartment (Fig. 4). Compared to the uniformed model, first peak prediction accuracy increased by 51% in the medial compartment and 30% in the lateral compartment when the fully-informed model was used (Fig. 5).

The contact force predictions from the fully-informed model were statistically similar to the *in-vivo* measurements for each peak in both the medial and lateral compartments; predictions from the uniformed model were only statistically similar for the second peak in the medial compartment (Table 1). Over the stance phase, predictions from the fully-informed, uniformed, alignment-informed, and contact-point-informed models had RMSE of 220N, 332N, 241N, and 297N, respectively.

Specifying a more valgus alignment decreased medial compartment force and increased lateral compartment force (Fig. 6). Specifying a medial shift of the contact locations had the same effect. We found that each additional degree of tibiofemoral valgus alignment decreased the first peak of the medical contact force by 51N and increased the first peak of the lateral contact force by 30N ($r^2=0.99$). Translating the contact point locations medially

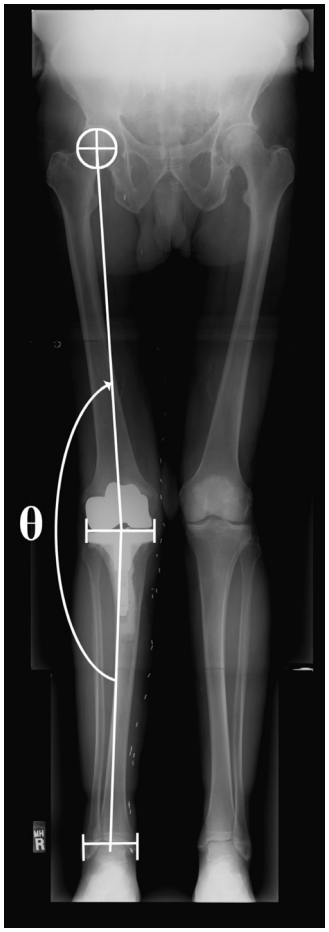

Fig. 2. Anterioposterior radiograph of the participant's lower-extremity used to determine the subject-specific alignment for the musculoskeletal model. Angle θ (174°) was found by drawing lines connecting the hip, knee, and ankle joint centers, which were defined as the center of the femoral head, center of the femoral condyles, and midpoint of the medial and lateral margins of the ankle, respectively.

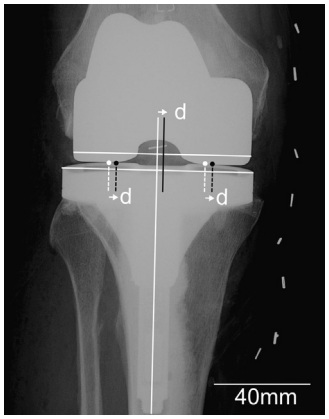

Fig. 3. The anterioposterior radiograph of the participant's instrumented (right) knee that was used to determine the frontal-plane location of the femoral implant component relative to the tibial implant component. The parameter, d, was measured as the distance between the centerlines of each component (3 mm). A measurement scale was set from the known width of the implant. In the model, we specified the subject-specific medial/lateral compartment contact locations (black dots) by shifting the generic medial/lateral locations (white dots) medially by d, thus maintaining an intercondylar distance of the instrumented implant. Therefore, for the fully-informed model and contact-point-informed model, the medial compartment point of contact was located 23 mm medial of the knee joint center, while the lateral compartment point of contact was located 17 mm lateral of the knee joint center.

by 1 mm decreased the first peak of the medial contact force by 41N and increased the first peak lateral compartment contact force by 33N ($r^2=0.99$); translating the contact point locations laterally by 1 mm had the opposite effect.

Muscle forces were the primary contributor to the knee joint contact force. For the fully-informed model, the sum of the muscle forces crossing the knee was 903N at the first peak of knee loading and 853N at the second peak. The sum of the muscle forces crossing the knee were not significantly different between model conditions. Individual peak muscle forces were similar between model conditions for all muscles except for the tensor-fasciae-latae, which increased from 62N in the uniformed model condition to 82N in the alignment-informed and fully-informed model conditions.

4. Discussion

We developed a novel, configurable knee joint in a full body musculoskeletal model that simplifies the prediction of medial/lateral tibiofemoral contact forces during locomotion, fulfilling the first goal of this study. This model allows investigators to specify subject-specific joint alignment and compartment contact locations to more accurately estimate tibiofemoral contact forces in individuals with non-neutral alignment.

The second goal of this study was to quantify the prediction accuracy of knee contact forces in an individual with non-neutral tibiofemoral alignment using our model with generic geometric parameters *versus* our model with subject-specific parameters. We found that prediction accuracy was improved by specifying each subject-specific parameter. However, predictions for all model conditions had limited accuracy during early stance (Fig. 4). Since muscles crossing the knee are not producing relatively large forces during this interval (*e.g.* summed muscle forces were <405N at 10% of stance), the predictions appear sensitive to small errors in the frontal-plane application of the external forces. During mid-stance, the lateral contact force was under-predicted for all models. Our objective function, which minimizes muscle activation and produces low levels of muscle co-contraction, may contribute to the reduced mid-stance accuracy since significant levels of co-contraction has been reported in older adults during mid-stance (Schmitz et al., 2009). Furthermore, we selected static optimization weighting factors that minimized the first and second peak error, but not mid-stance error. Therefore, our results were not optimized for this portion of the gait cycle.

The third goal of this study was to investigate how geometric parameters, in particular tibiofemoral alignment and contact locations, affect estimates of medial/lateral contact forces. Our results indicate that frontal-plane tibiofemoral alignment is an important model parameter when predicting medial/lateral compartment contact forces. Hast et al. predicted medial/lateral contact forces from the same subject and dataset used in our study, but did not report incorporating subject-specific frontal-plane alignment (Hast and Piazza, 2013). Acknowledging that they used a different approach to estimate muscle and contact forces, they reported larger medial contact forces and smaller lateral contact forces compared to the *in-vivo* data. Their results resemble our predictions from our model with neutral alignment. Specifying subject-specific tibiofemoral alignment may therefore improve estimates of medial/lateral contact forces from other approaches that rely on knee models with a constrained abduction-adduction DOF. Thelen et al. report that small variations in tibiofemoral alignment ($\pm 2°$) in their dynamic contact model altered the medial-lateral distribution by up to 12% (Thelen et al., 2014), suggesting that specification of subject-specific alignment would be important in this type of model as well.

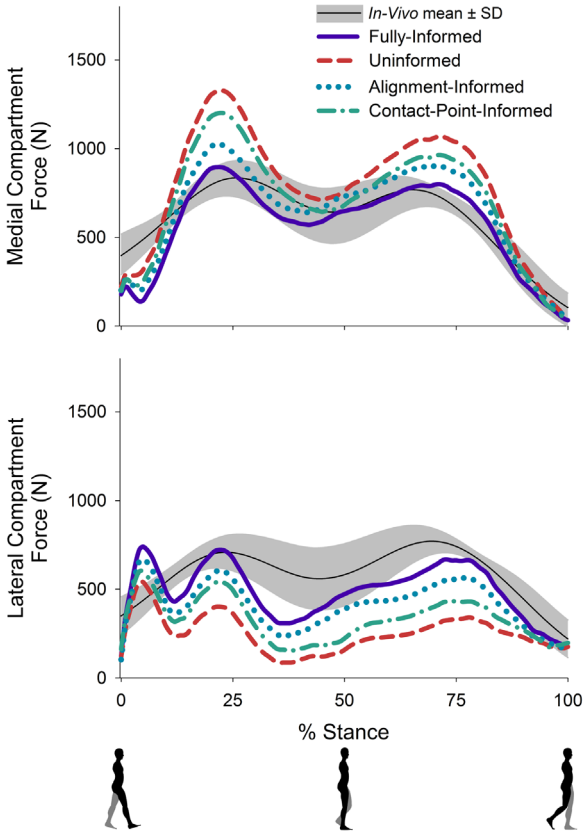

Fig. 4. Medial (top) and lateral (bottom) compartment tibiofemoral contact forces during stance measured *in-vivo* from the instrumented implant (skinny black line) and predicted using the fully-informed (purple, solid line), uninformed (red, dashed line), alignment-informed (blue, dotted line), and contact-point-informed (green, dash-dot line) models.

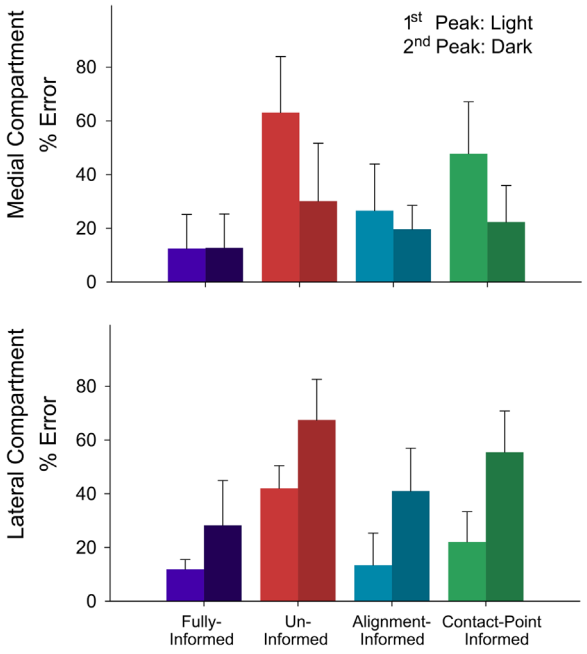

Fig. 5. Percent error in first (light) and second (dark) peak medial (top) and lateral (bottom) tibiofemoral contact forces between the *in-vivo* measurements from the instrumented implant and the fully-informed (purple), uninformed (red), alignment-informed (blue), and contact-point-informed (green) models. Error bars represent 1 standard deviation (SD).

Table 1
95% Confidence Intervals (CI) of the medial and lateral compartment first and second peak contact forces for the *in-vivo* data measured from the instrumented implant and each model condition. Bolded entries denote 95% CIs for the model predictions that do not overlap with the 95% CI for the *in-vivo* data (indicating significant difference).

	First peak (N)		Second peak (N)	
	Medial	Lateral	Medial	Lateral
In-Vivo	679–991	556–871	695–871	657–911
Fully-informed	827–1002	635–825	559–987	399–714
Uniformed	**1234–1461**	**319–502**	786–1244	**85–417**
Alignment-informed	951–1139	531–689	648–1095	**302–612**
Contact-point-informed	**1119–1322**	439–663	703–1136	**183–507**

Predictions of medial/lateral tibiofemoral contact forces were directly proportional to model-specified frontal-plane alignment (Fig. 6). This relationship is supported by findings from a study with five individuals with instrumented knee implants and a range of post-operative lower-extremity alignments (Halder et al., 2012). Thirty percent of total knee replacement cases result in postoperative alignment beyond $\pm 3^{\circ}$ varus-valgus (Bäthis et al., 2004), while the standard deviations of tibiofemoral alignment are 3° in healthy individuals and 8° in osteoarthritic individuals (Cooke et al., 1997). A 3° difference between model and subject alignment would alter first peak medial contact force predictions by 23% of body-weight and lateral contact force predictions by 14% of body-weight. Researchers can likely improve contact force estimates by utilizing subject-specific knee alignment acquired from radiographic images.

Our model resolved medial/lateral compartment loads by approximating them as though they occurred at single points of contact. We estimated these contact locations from an anterioposterior knee radiograph with knowledge of the intercondylar distance (40 mm) determined from a similar implant (Zhao et al., 2007). Since a non-neutral lower-extremity may influence the relative placement of the femoral and tibial prosthesis components, we analyzed a radiograph of the subject's instrumented knee. We found a medial shift of the femoral component relative to the tibial component. Therefore, we shifted the medial/lateral locations in our model accordingly, while maintaining the previously reported intercondylar distance. It has been reported that medial/lateral contact points deviate in the medial-lateral direction up to ± 2.6 mm in artificial knee joints during walking (Zhao et al., 2007); therefore, we investigated the sensitivity of model predictions across a similar range (± 4 mm). Tibiofemoral contact forces were directly proportional to the specified contact locations. A 2 mm difference between model and subject contact-locations alters the predicted first peak of the medial contact force by 12% of body-weight and lateral contact force 10% of body-weight. We recommend that estimates of condylar contact based on center of pressure be used when this model is applied to biological knees.

Tibiofemoral alignment and contact locations primarily affected the medial-lateral load distribution by altering how the external loads and muscle forces passed relative to each compartment in the frontal-plane. In model conditions with subject-specific alignment, the knee joint moved medially causing the external knee adduction moment to decrease. Similarly, in model conditions with subject-specific contact locations, the contact locations shifted medially causing the external adduction moment relative to each compartment to decrease. In both cases, a reduced adduction moment from the external forces increased the lateral compartment contact force and decreased the medial compartment contact force. Altering the frontal-plane compartment contact locations also affected the frontal-plane muscle moment arms about each compartment. A medial shift in the contact location caused the muscle forces to

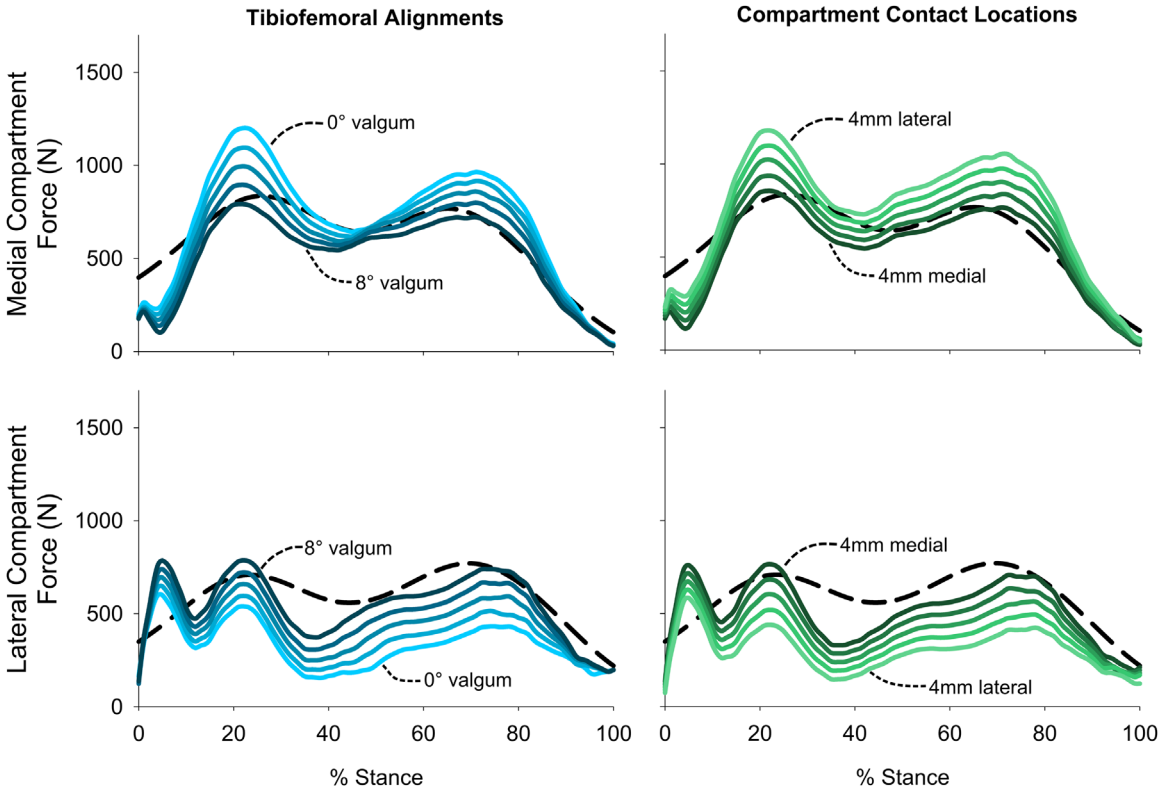

Fig. 6. Effects of model-specified alignment (left), and compartment contact locations (right) on medial compartment (top) and lateral compartment (bottom) tibiofemoral contact forces during stance. The black-dashed lines represent the *in-vivo* measurements. Deviation of model-specified tibiofemoral alignment from 8° genu valgum (dark blue) to generic alignment (0° genu valgum, light blue), at 2° increments. Deviation of compartment contact locations from 4 mm medial (dark green) to 4 mm lateral (light green), at 2 mm increments.

increase their contribution to lateral compartment loading and decrease their contribution to medial compartment loading.

There are several limitations of this study. First, we were restricted to data from only a single individual because the design of our study necessitated a subject with an instrumented knee implant, post-operative non-neutral alignment, and radiographic images. Since we found directly proportional relationships between model-predictions and the geometric parameters, our results may apply across a range of individuals. Second, an assumption of our model was that tibiofemoral contact acted through single points in each compartment and the locations of these points relative to the tibia reference frame remained stationary. The impact of this assumption is thought to be small since reports of the *in-vivo* frontal-plane medial/lateral contact locations from dual-orthogonal fluoroscopy and magnetic resonance images were not significantly different between 0° and 30° of weight-bearing knee flexion (Li et al., 2005). Third, we used a weighted static optimization approach to determine muscle weighting factors rather than an EMG driven approach. However, we found that the predicted medial-lateral distribution for each model and alignment condition were insensitive to variation of muscle weighting factors in static optimization. Since we applied the same objective function across all model conditions, our conclusions regarding the effect of the geometric parameters on model predictions are unlikely to depend on the method used to resolve muscle forces.

This study provides a novel articulating model of the knee to be used within a full-body musculoskeletal model with load bearing medial/lateral compartment joint structures for the prediction of these loads. For the participant in our study with genu valgum, specifying subject-specific lower-extremity alignment and medial/lateral compartment contact locations estimated from a standing anterior-posterior radiograph improved predictions of medial/lateral tibiofemoral contact forces. This suggests that frontal-plane alignment and frontal-plane medial/lateral compartment contact locations are important subject-specific model parameters that should be incorporated when predicting medial/lateral contact forces.

Conflict of interest statement

The authors declare no conflict of interest.

Acknowledgments

We thank the individuals associated with the Knee Load Grand Challenge, in particular B.J. Fregly, PhD and Darryl D'Lima, MD, PhD, and the OpenSim project for their contributions to these valuable data-sets and tools. This work was supported by NIH Grants R24 HD065690 and F31 HD080261.

References

Bäthis, H., Perlick, L., Tingart, M., Lüring, C., Zurakowski, D., Grifka, J., 2004. Alignment in total knee arthroplasty: a comparison of computer-assisted surgery with the conventional technique. J. Bone Joint Surg. Brit. Vol. 86-B, 682–687.

Bei, Y., Fregly, B.J., 2004. Multibody dynamic simulation of knee contact mechanics. Med. Eng. Phys. 26, 777–789.

Cooke, D., Scudamore, A., Li, J., Wyss, U., Bryant, T., Costigan, P., 1997. Axial lower-limb alignment: comparison of knee geometry in normal volunteers and osteoarthritis patients. Osteoarthr. Cartil. 5, 39–47.

Delp, S.L., Anderson, F.C., Arnold, A.S., Loan, P., Habib, A., John, C.T., Guendelman, E., Thelen, D.G., 2007. OpenSim: open-source software to create and analyze dynamic simulations of movement. IEEE Trans. Biomed. Eng. 54, 1940–1950.

Delp, S.L., Loan, J.P., Hoy, M.G., Zajac, F.E., Topp, E.L., Rosen, J.M., 1990. An interactive graphics-based model of the lower extremity to study orthopaedic surgical procedures. IEEE Trans. Biomed. Eng. 37, 757–767.
DeMers, M.S., Pal, S., Delp, S.L., 2014. Changes in tibiofemoral forces due to variations in muscle activity during walking. J. Orthop. Res. 32, 769–776.
Dillon, C.F., Rasch, E.K., Gu, Q., Hirsch, R., 2006. Prevalence of knee osteoarthritis in the United States: arthritis data from the third national health and nutrition examination survey 1991-94. J. Rheumatol. 33, 2271–2279.
Fregly, B.J., Besier, T.F., Lloyd, D.G., Delp, S.L., Banks, S.A., Pandy, M.G., D'Lima, D.D., 2012. Grand challenge competition to predict *in vivo* knee loads. J. Orthop. Res. 30, 503–513.
Gerus, P., Sartori, M., Besier, T.F., Fregly, B.J., Delp, S.L., Banks, S.A., Pandy, M.G., D'Lima, D.D., Lloyd, D.G., 2013. Subject-specific knee joint geometry improves predictions of medial tibiofemoral contact forces. J. Biomech. 46, 2778–2786.
Halder, A., Kutzner, I., Graichen, F., Heinlein, B., Beier, A., Bergmann, G., 2012. Influence of limb alignment on mediolateral loading in total knee replacement: *in vivo* measurements in five patients. J. Bone Joint Surg. 94, 1023–1029.
Hast, M.W., Piazza, S.J., 2013. Dual-joint modeling for estimation of total knee replacement contact forces during locomotion. J. Biomech. Eng. 135, 021013.
Herzog, W., Longino, D., Clark, A., 2003. The role of muscles in joint adaptation and degeneration. Langenbeck's Archives Surg. 388, 305–315.
Hsu, R.W., Himeno, S., Coventry, M.B., Chao, E.Y., 1990. Normal axial alignment of the lower extremity and load-bearing distribution at the knee. Clin. Orthop. Relat. Res 255, 215–227.
Hurwitz, D.E., Ryals, A.B., Case, J.P., Block, J.A., Andriacchi, T.P., 2002. The knee adduction moment during gait in subjects with knee osteoarthritis is more closely correlated with static alignment than radiographic disease severity, toe out angle and pain. J. Orthop. Res. 20, 101–107.
Kumar, D., Rudolph, K.S., Manal, K.T., 2012. EMG-driven modeling approach to muscle force and joint load estimations: Case study in knee osteoarthritis. J. Orthop. Res. 30, 377–383.
Lerner, Z.F., Haight, D.J., Demers, M.S., Board, W.J., Browning, R.C., 2013. The effects of walking speed on tibiofemoral loading estimated via musculoskeletal modeling. J. Appl. Biomech 30, 197–205.
Li, G., DeFrate, L.E., Park, S.E., Gill, T.J., Rubash, H.E., 2005. *In Vivo* articular cartilage contact kinematics of the knee: an investigation using dual-orthogonal fluoroscopy and magnetic resonance image–based computer models. Am. J. Sports Med. 33, 102–107.
Lin, Y.-C., Walter, J.P., Banks, S.A., Pandy, M.G., Fregly, B.J., 2010. Simultaneous prediction of muscle and contact forces in the knee during gait. J. Biomech. 43, 945–952.
Meyer, A.J., D'Lima, D.D., Banks, S.A., Coburn, J., Harman, M., Mikashima, Y., Fregly, B.J., 2001. Evaluation of regression equations for medial and lateral contact force from instrumented knee implant data. ASME Summer Bioengineering Conference.
Moreland, J.R., Bassett, L.W., Hanker, G.J., 1987. Radiographic analysis of the axial alignment of the lower extremity. J. Bone Joint Surg. 69, 745–749.
Morrison, J.B., 1970. The mechanics of the knee joint in relation to normal walking. J. Biomech. 3, 51–61.
Ritter, M.A., Faris, P.M., Keating, E.M., Meding, J.B., 1994. Postoperative alignment of total knee replacement. Its effect on survival. Clin. Orthop. Relat. Res 299, 153–156.
Schmitz, A., Silder, A., Heiderscheit, B., Mahoney, J., Thelen, D.G., 2009. Differences in lower-extremity muscular activation during walking between healthy older and young adults. J. Electromyography Kinesiol. 19, 1085–1091.
Sharma, L., Hurwitz, D., Thonar, E., Sum, J., Lenz, M., Dunlop, D., 1998. Knee adduction moment, serum hyaluronan level, and disease severity in medial tibiofemoral osteoarthritis. Arthr. Rheumatol. 41, 1233–1240.
Sharma, L., Song, J., Felson, D.T., Cahue, S., Shamiyeh, E., Dunlop, D.D., 2001. The role of knee alignment in disease progression and functional decline in knee osteoarthritis. J. Am. Med. Association 286, 188–195.
Steele, K.M., DeMers, M.S., Schwartz, M.H., Delp, S.L., 2012. Compressive tibiofemoral force during crouch gait. Gait Posture 35, 556–560.
Thelen, D.G., Choi, K.W., Schmitz, A.M., 2014. Co-simulation of neuromuscular dynamics and knee mechanics during human walking. J. Biomech. Eng. 136, 021033.
Winby, C.R., Lloyd, D.G., Besier, T.F., Kirk, T.B., 2009. Muscle and external load contribution to knee joint contact loads during normal gait. J. Biomech. 42, 2294–2300.
Yang, N.H., Nayeb-Hashemi, H., Canavan, P.K., Vaziri, A., 2010. Effect of frontal plane tibiofemoral angle on the stress and strain at the knee cartilage during the stance phase of gait. J. Orthop. Res. 28, 1539–1547.
Zhao, D., Banks, S.A., D'Lima, D.D., Colwell, C.W., Fregly, B.J., 2007. *In vivo* medial and lateral tibial loads during dynamic and high flexion activities. J. Orthop. Res. 25, 593–602.